Effects of Surfactant Adsorption on Electro-osmotic Flow in Electro-kinetic Soil Remediation

Zhenlei Zhang [1], Lei Zhu [2], and Yudou Wang [1, *]

[1] College of Science, China University of Petroleum (East China), Qingdao, Shandong, China;

[2] School of Materials Science and Engineering, China University of Petroleum (East China), Qingdao, Shandong, China.

Abstract. This study investigates the impact of surfactant adsorption on electro-osmotic flow in a solid-liquid interface for electro-kinetic soil remediation. The surfactant saturation process and its effects on EOF were simulated by solving the Poisson-Nernst-Planck equation, the convective diffusion equation, and the Navier-Stokes equation. Results indicate that surfactant saturation significantly alters electro-osmotic flow velocity profiles, with the flow transitioning from a Poiseuille-like pattern to a uniform, piston-like profile as the surfactant concentration increases. The enhanced electroosmotic flow, driven by increased zeta potential on the channel wall, improves contaminant mobilization and transport. These findings suggest that surfactant-enhanced electro-osmotic flow can optimize electro-kinetic soil remediation by improving fluid and contaminant movement, offering potential for more efficient and faster soil decontamination, particularly in heterogeneous soil conditions.

Keywords: surfactant; electro-kinetics; electroosmotic flow; soil remediation; zeta potential.

1. Introduction

Electro-kinetic soil remediation (EKR) is an increasingly significant technique for the in-situ treatment of contaminated soils, providing an environmentally friendly and cost-effective alternative to traditional soil remediation methods [1,2]. By applying an external electric field, EKR facilitates the movement of charged contaminants toward the electrodes, thereby enhancing their removal and promoting soil decontamination. The electro-osmotic flow (EOF), which is generated by the application of an electric field, plays a crucial role in this process by driving the movement of fluid through the soil matrix, thus aiding the migration of pollutants toward the electrodes for subsequent removal. To enhance the effectiveness of EKR, the incorporation of surfactants has garnered attention in recent years. Surfactants can significantly improve the remediation process through several mechanisms, including aiding in the mobilization and solubilization of hydrophobic pollutants, enhancing the desorption rate of pollutants from soil particles by altering soil-pollutant interactions, and facilitating the migration of micelles that encapsulate contaminants through the soil [3,4]. However, despite the clear potential of surfactants to enhance EKR, relatively few studies have investigated their impact on EOF during the remediation process. Understanding how surfactants affect EOF could provide deeper insights into optimizing the use of surfactants in electro-kinetic applications, helping to balance the effects on pollutant transport and EOF-driven fluid movement within the soil. Given the limited research in this area, further exploration of the relationship between surfactant properties, EOF, and contaminant removal is essential to fully leverage the benefits of surfactant-enhanced EKR[5].

The most prominent feature of surfactants lies in their propensity to adsorb at interfaces, thereby markedly modifying interfacial characteristics such as wettability and surface charge [6]. Previous studies have demonstrated that surfactant adsorption exerts a strong impact on the zeta potential, which not only governs the electroosmotic flow (EOF) mobility but also serves as an indicator of interfacial charge density. Khademi [7] investigated the zeta potential of polymethyl methacrylate (PMMA) in contact with different surfactant solutions and reported distinct responses arising from diverse adsorption mechanisms. Similarly, Azadi [8] explored the effect of surfactant coatings on EOF behavior in a PMMA matrix in the presence of surfactants. This investigation revealed that the adsorption and interactions of surfactants with the PMMA surface significantly impact the rate of

EOF by altering the net surface charge density. It is important to note that the adsorption of surfactants at the solid-liquid interface is time-dependent and highly susceptible to hydrodynamic conditions. Consequently, accurately characterizing the impact of the instantaneous adsorption process on EOF cannot be achieved through experimental approaches.

Numerical simulation methods provide a valuable approach to investigate the detailed EOF behavior. In the context of the EDL potential distribution, the Boltzmann distribution is commonly assumed to describe the ionic distribution under thermodynamic equilibrium [9,10]. However, it is important to note that the steady-state assumption fails to account for the influence of transient surfactant adsorption on flow behavior. To gain a more comprehensive understanding of the role of surfactant adsorption in fluid dynamics, this study employs numerical simulations to analyze surfactant transport in a microchannel subjected to an external electric field and a pressure gradient. The adsorption and desorption dynamics of surfactants are described using a first-order reaction governed by the Langmuir model. The analysis systematically investigates how adsorption kinetics affect both fluid flow and surfactant transport.

2. Problem STATEMENT and numerical APPROACH

We investigate surfactant transport in a microchannel subjected to an externally imposed electric field and a pressure gradient. The system configuration is illustrated in Fig. 1. The computational domain consists of a parallel-plate microchannel with a length of $w = 14\mu m$ and a height of $H = 4\mu m$. At the inlet, the surfactant solution is introduced at a constant concentration of $c_{s,in} = 0.4 mol/m^3$, while the channel is initially filled with a NaCl solution at a concentration of $c_0 = 0.25 mol/m^3$. Fluid motion is driven simultaneously by the applied electric field E and the imposed pressure difference. The electric potential at the microchannel walls is set to $\xi = -36.7 mV$. Upon entering the microchannel, surfactant molecules may adsorb onto available surface sites, with a maximum adsorption capacity of $c_{s0} = 1.2 \times 10^{-4} mol/m^2$.

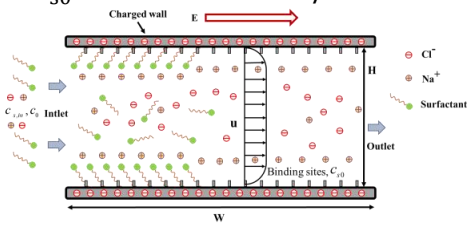

Figure. 1 Geometry of the simulation domain used in this study.

The coupled system governing fluid flow and surfactant transport in the microchannel consists of the Laplace equation for the external electric field (Eq. (1)), the Poisson equation for the internal potential in the presence of the EDL (Eq. (2)), the convection–diffusion equation for surfactant transport (Eq. (3)), the Poisson–Nernst–Planck equations for ion distributions (Eqs. (4)–(5)), and the Navier–Stokes equation for fluid velocity (Eq. (6)).The equations mentioned are as follows [5,11,12]:

$$\nabla^2 \psi = 0. \tag{1}$$

$$\nabla^2 \varphi = -\frac{F}{\varepsilon_0 \varepsilon_r}(z^+ c_+ + z^- c_-). \tag{2}$$

$$\frac{\partial c}{\partial t} + \nabla \cdot (uc) = \nabla \cdot (D_s \nabla c). \tag{3}$$

$$\frac{\partial c_+}{\partial t} + \nabla \cdot \left[uc_+ - D_\pm \nabla c_+ - \frac{z_+ e c_+ D_\pm}{k_B T} \nabla(\varphi + \psi) \right] = 0. \tag{4}$$

$$\frac{\partial c_-}{\partial t} + \nabla \cdot \left[uc_- - D_\pm \nabla c_- - \frac{z_- e c_- D_\pm}{k_B T} \nabla(\varphi + \psi) \right] = 0. \tag{5}$$

$$\rho \frac{\partial u}{\partial t} + \rho(u \cdot \nabla)u = \nabla \cdot \left[-pI + \mu(\nabla u + (\nabla u)^T) - \frac{2}{3}\mu(\nabla \cdot u)I \right] + F. \tag{6}$$

Here, u is the fluid velocity, p is the pressure, ρ is the density, t is the time, I is the unit vector, μ presents the dynamic viscosity, F is the body force. ψ is the potential of externally applied electric field, while φ represents the intrinsic potential induced by surface charges. ε_r and ε_0 are the relative permittivity of the solution and the permittivity of vacuum, respectively. c_- and c_+ are the concentrations of negative and positive ions, with z^+ (z^-) representing their respective charge numbers, and $D_\pm$ is the ionic diffusion coefficient. F is the Faraday constant. D_s is the surfactant diffusion coefficient. c is the surfactant concentration. Furthermore, e denotes the elementary electric charge, T is the absolute temperature, and k_B is Boltzmann constant. In this study, the Langmuir adsorption model [13] is employed to describe the surfactant adsorption process. To capture its effect on the flow field, it is necessary to establish the relationship between the surface-bound surfactant concentration and the zeta potential (ZP). By interpolating experimental data reported in reference [5,7], the complete functional dependence of ZP on the surface-bound surfactant concentration was obtained.

3. Results and discussions

To investigate the effect of surfactant adsorption–desorption at the solid–liquid interface on EOF, this section comprehensively analyzes the entire process of surfactant transport and the resultant variations in EOF. Firstly, the surfactant transport process is illustrated in the Fig.2. As shown in Fig.2, surfactant enters from the left inlet and gradually flows towards the outlet over time. As evident from the contour lines in the figure ($t = 1.5$ ms and $t = 6.0$ ms), the concentration is higher in the middle of the channel compared to the solid-liquid interface, resulting in a "Poiseuille-like" contour profile. Initially, the adsorption process primarily occurs near the entrance, resulting in the highest concentration at this location. Initially, the surfactant concentration is highest near the channel inlet due to the dominant adsorption process. As time progresses, the adsorption front propagates downstream, and at later times, the upstream region reaches saturation.

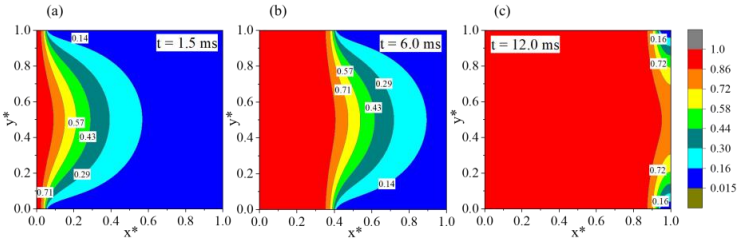

Figure. 2 Non-dimensional surfactant concentration distributions at various time instances.

Adsorption of surfactant molecules at the microchannel walls leads to a gradual increase in surface-bound surfactant concentration. As shown in Fig. 3(a), adsorption initially occurs near the inlet, producing the highest concentration locally, and progressively extends downstream until the upstream region saturates. The surface-bound concentration strongly modulates the zeta potential, as illustrated in Fig. 3(b). Surfactant introduction markedly increases the absolute value of the zeta potential, indicating a direct correlation between higher surface-bound surfactant concentrations and larger zeta potential magnitudes.

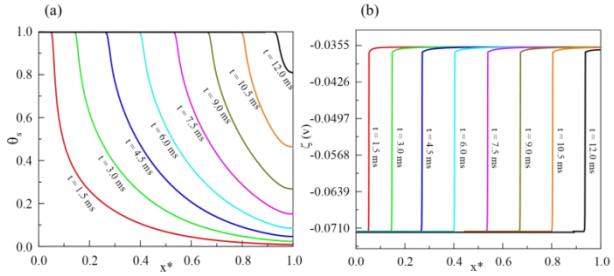

Figure. 3 (a) Temporal evolution of the dimensionless surface-bound surfactant concentration and (b) zeta potential in the wall surface.

Fig.4 illustrates the profiles of the x-component of fluid velocity across the channel cross-section before and after surfactant adsorption reaches saturation. The results clearly show that prior to surfactant saturation, the electroosmotic velocity is lower than the hydrodynamic velocity, resulting in velocity profiles that closely resemble Poiseuille flow. This suggests that, in the absence of significant surfactant adsorption, the electro-osmotic flow is relatively weak, and the primary driver for fluid movement is hydrodynamic forces rather than electrokinetic effects. However, as surfactant adsorption increases and reaches a point of saturation, the electroosmotic effect on the channel wall becomes more pronounced, as evidenced by the development of a piston-like velocity profile at $t = 7$ ms. This transition signifies a shift in the dominant forces driving flow, where the EOF begins to enhance the overall fluid movement significantly. Once saturation is achieved, the electroosmotic velocity surpasses the hydrodynamic velocity, demonstrating that the electroosmotic force becomes the primary driver for fluid and contaminant transport.

In the context of EKR, this behavior is particularly significant. The enhanced EOF facilitated by surfactants can lead to more efficient contaminant mobilization and transport, improving the overall remediation process. By accelerating the movement of fluids and pollutants toward the electrodes, the surfactant-induced EOF may reduce the overall time required for decontamination and increase the effectiveness of pollutant removal. This finding underscores the importance of optimizing surfactant concentrations to achieve maximum EOF enhancement, which could be key to improving the efficiency of EKR applications.

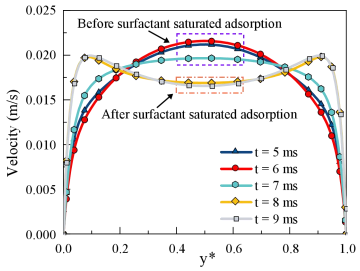

Figure. 4 Profiles of the x-component of fluid velocity across the channel cross-section.

Surfactant concentration strongly influences adsorption kinetics and, consequently, fluid flow. As shown in Fig. 5(a), higher surfactant concentrations expand the saturation region of surface-bound surfactants. The results indicate that increased concentrations enhance the adsorption rate at the solid–liquid interface by providing more molecules for adsorption. Figure 5(b) further shows that the time required to reach saturation decreases as surfactant concentration increases.

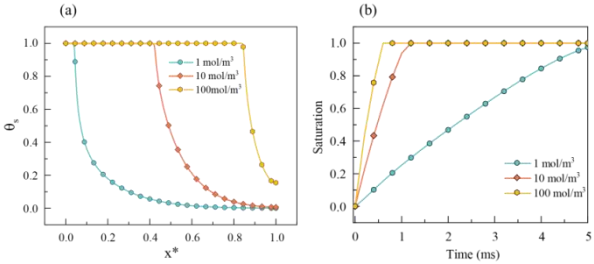

Figure. 5 Effects of surfactant concentration on non-dimensional surface-bound surfactant concentration (a) and saturation (b).

The results presented in Fig.6 further emphasize the significant influence of surfactant concentration on EOF behavior within the channel. As the surfactant concentration increases, the velocity profile transitions towards a more pronounced piston-type flow, indicating that the flow is becoming increasingly uniform across the channel. This uniformity is critical, as it suggests a more efficient and homogeneous fluid movement, which is beneficial for contaminant transport during EKR. At a surfactant concentration of $c_{s,in} = 100\text{mol/m}^3$, the velocity distribution across the entire channel length adopts a consistent piston-like pattern. This trend directly reflects the distribution of surface-bound surfactant concentration illustrated in Fig.5(a), where most of the

channel surface is saturated with surfactants. The widespread adsorption of surfactants enhances the electroosmotic flow by increasing the electroosmotic effect on the channel walls, resulting in the uniform, piston-like flow observed.

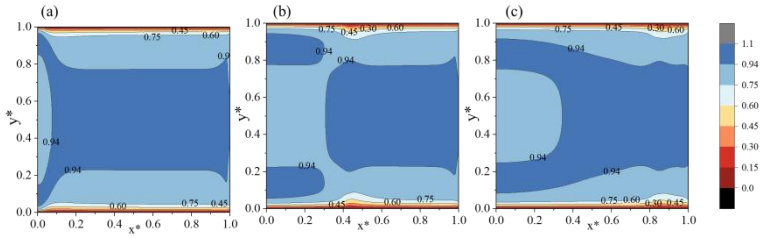

Figure. 6 Profiles of non-dimensionalized velocity with different surfactant concentrations.

The uniform flow pattern driven by the surfactant-induced EOF ensures that contaminants are transported more evenly across the soil matrix, improving the effectiveness of contaminant extraction. The enhanced mobilization and transport of pollutants could lead to faster decontamination times and better utilization of the applied electric field, optimizing the efficiency of the EKR process. Therefore, increasing surfactant concentration not only improves EOF but also ensures that the fluid movement is more homogenous, which could be a key factor in improving the scalability and effectiveness of EKR applications, particularly in soils with heterogeneous properties.

4. Summary

This study investigates the impact of surfactant adsorption dynamics on EOF at a solid-liquid interface. The saturation process of surfactant in the channel and its subsequent influence on EOF were numerically simulated. Results show that surfactant saturation significantly alters EOF velocity profiles. Before saturation, EOF resembles Poiseuille flow, but after saturation, the zeta potential increases, enhancing EOF velocity. The velocity profile of saturated surfactant adsorption adopts a piston-like flow, with increased surfactant concentration leading to a more uniform flow across the channel. These findings demonstrate that surfactant-enhanced EOF improves contaminant transport and mobilization, potentially optimizing EKR. The study highlights the role of surfactant concentration in enhancing EOF, offering insights for more efficient soil decontamination, particularly in heterogeneous soils. This research provides a basis for developing tailored remediation strategies to accelerate and enhance EKR processes.

References

[1] Ghazanfari E, Shrestha RA, Miroshnik A, Pamukcu S. Electrically assisted liquid hydrocarbon tr ansport in porous media. Electrochimica Acta 2012;86:185–91. https://doi.org/10.1016/j.electacta.2 012.04.077.

[2] Pamukcu S, Shrestha RA, Ribeiro AB, Mateus EP. Electrically induced displacement transport o f immiscible oil in saline sediments. Journal of Hazardous Materials 2016;313:185–92. https://doi. org/10.1016/j.jhazmat.2016.04.005.

[3] Li Y, Jiang L. Comparison of the crude oil removal effects of different surfactants in electrokin etic remediation of low-permeability soil. Journal of Environmental Chemical Engineering 2021;9: 105190. https://doi.org/10.1016/j.jece.2021.105190.

[4] Ansari A, Haroun M, Sayed NA, Kindy NA, Ali B, Shrestha RA, et al. A New Approach Opt imizing Mature Waterfloods with Electrokinetics-Assisted Surfactant Flooding in Abu Dhabi Car bonate Reservoirs. All Days, Kuwait City, Kuwait: SPE; 2012, p. SPE-163379-MS. https://doi.or g/10.2118/163379-MS.

[5] Zhang Z, Gao M, Sun Z, Zhou W, Wang D, Zhu L, et al. Analysis of surfactant transport und er combined electroosmotic and pressure-driven flow in microchannel with consideration of adso

rption kinetics. International Communications in Heat and Mass Transfer 2025;168:109462. https://doi.org/10.1016/j.icheatmasstransfer.2025.109462.

[6] Tsagkaropoulou G, Allen FJ, Clarke SM, Camp PJ. Self-assembly and adsorption of cetyltrimethylammonium bromide and didodecyldimethylammonium bromide surfactants at the mica–water interface. Soft Matter 2019;15:8402–11. https://doi.org/10.1039/C9SM01464K.

[7] Khademi M, Wang W, Reitinger W, Barz DPJ. Zeta Potential of Poly(methyl methacrylate) (PMMA) in Contact with Aqueous Electrolyte–Surfactant Solutions. Langmuir 2017;33:10473–82. https://doi.org/10.1021/acs.langmuir.7b02487.

[8] Azadi G, Tripathi A. Surfactant-induced electroosmotic flow in microfluidic capillaries. ELECTROPHORESIS 2012;33:2094–101. https://doi.org/10.1002/elps.201100633.

[9] Mondal S, De S. Mass transport in electrokinetic microflows with the wall reaction affecting the hydrodynamics. Theoretical and Computational Fluid Dynamics 2021;35:39–60. https://doi.org/10.1007/s00162-020-00549-5.

[10] Talapatra S, Chakraborty S. Double layer overlap in ac electroosmosis. European Journal of Mechanics - B/Fluids 2008;27:297–308. https://doi.org/10.1016/j.euromechflu.2007.06.005.

[11] Yang X, Shi B, Chai Z, Guo Z. A Coupled Lattice Boltzmann Method to Solve Nernst–Planck Model for Simulating Electro-osmotic Flows. J Sci Comput 2014;61:222–38. https://doi.org/10.1007/s10915-014-9820-6.

[12] Boyer F, Lapuerta C, Minjeaud S, Piar B, Quintard M. Cahn–Hilliard/Navier–Stokes Model for the Simulation of Three-Phase Flows. Transp Porous Med 2010;82:463–83. https://doi.org/10.1007/s11242-009-9408-z.

[13] Brigodiot C, Marsiglia M, Dalmazzone C, Schroën K, Colin A. Studying surfactant mass transport through dynamic interfacial tension measurements: A review of the models, experiments, and the contribution of microfluidics. Advances in Colloid and Interface Science 2024;331:103239. https://doi.org/10.1016/j.cis.2024.103239.